Euronoise 2018
Crete

# Modal analysis and flanking sound insulation in connected panels of cross-laminated-timber at low frequencies

Blasius Buchegger
Laboratory for Building Science, University of Technology, Graz, Austria.
Heinz Ferk
Laboratory for Building Science, University of Technology, Graz, Austria.
Martin Schanz
Institute of Applied Mechanics, University of Technology, Graz, Austria.

**Summary**

Improving the flanking sound insulation performance of timber based constructions at low frequencies is a big challenge, mostly caused by the low mass of the material timber. Additional linings on the walls increase the sound insulation, but in most cases, the effect of this measure is strongly limited to lower frequencies above 100 Hz. However, there is a high potential to use the physical effect of modal decoupling to increase the flanking sound insulation especially for constructions of cross-laminated-timber at low and very low frequencies. Floors and walls are defined as single subsystems within a system of two coupled rooms. These subsystems only show local modes, if they are not connected to each other. In contrast, connected subsystems result in global modes of the overall system, if the individual local modes have similar eigenfrequencies. In this case, an excitation of a wall or a floor results in a high vibration response of the coupled wall. If the generation of these global modes is suppressed, the flanking sound insulation especially at low frequencies can be increased. This effect is studied in this contribution using validated numerical models based on the finite element method. Selected constructions have been chosen which are based on panels of cross-laminated-timber. Further, the results of 3D-models of coupled rooms are discussed. These results verify the applicability of this approach for common practical situations, and show the potential to obtain a basic sound insulation at low frequencies by a special design of cross-laminated-timber panels.

**PACS no. 43.20.Ks, 43.40.Dx, 43.40.Rj, 43.40.Ka**

## 1. Introduction

At the present time, the number of new timber-based multi-storey houses is growing in several countries worldwide. The usage of cross-laminated-timber is increasing due to several ecological and economical reasons and is also driven by the interesting mechanical performance of this material. Although the number of buildings is growing, two major challenges reduce the competitiveness of cross-laminated timber compared to massive construction methods like concrete or masonry: moisture sensitivity and sound insulation.

With regard to sound insulation, timber constructions often allow an advanced sound insulation at higher frequencies caused by, e.g., the high material damping. At low frequencies, timber constructions show a different behaviour caused by the low density that dominates the sound insulation. Additional linings on the walls or floors increase the sound insulation especially at frequencies above 100 Hz, but have less effect on the sound insulation at lower frequencies.

In Figure 1, results of standardized measurements [1] of the normalized impact sound pressure levels of various modifications of a cross-laminated timber floor construction are compared. Especially the typical shapes of the results show that the level increases with decreasing frequency. At low frequencies, plate resonances like bending modes are strongly excited caused by the low mass of the panel. Additional linings like a resilient layer and a floating floor or an additional suspended ceiling increases the sound insulation significantly, but have less influence below 100 Hz.

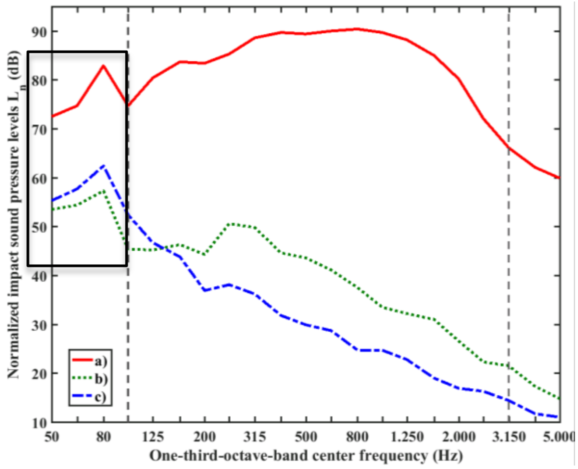


Figure 1. Comparison of floors – a) CLT, 5s, 140 mm b) Sit. a) with additional gravel filling, impact sound insulation and floating floor; c) Sit. b) with additional suspended ceiling

Improvements in the low frequency range may be archieved by adding mass, e.g. gravel fillings. But this measure decreases advantages of the construction material like low cost and fast mounting. Alternatively, additional impact sound insulation and a floating floor reduce the direct sound transmission. Additional resilient linings on the walls help to reduce flanking sound transmission. These measures are based on a decoupling effect of a resonating system with an eigenfrequency that sometimes coincide with the bending mode frequencies of the CLT-panels. As a consequence, resilient linings have no sufficient effect at low and very low frequencies, sometimes the sound insulation gets even worse there. Excitation by walking noise often results in a noise spectrum containing energy especially at low frequencies. This is caused by the wide impulse in the time domain which is a consequence of typical footgear used in dwellings. As a result, the modes of the panel are strongly excited and a high noise level occurs at single eigenfrequencies. In many cases this noise results in an annoying effect on neighbours because of its tonal character. During evaluations of noise immission, this tonal character can be taken into account by adding a surcharge of several decibels [2].

Alternatively, an improvement of the sound insulation can be reached by using special acoustic effects like modal (de-)coupling. Amongst others, flanking sound transmission – especially at low frequencies - is depending on the correlation of the vibration fields of the coupled panels. In general, every single panel shows eigenfrequencies and mode shapes that characterize the vibration behaviour of the component. The junction may couple these “local” mode shapes to “global” mode shapes, if two or more components have similar eigenfrequencies.

This principle can be shown using an advancement of the classical SEA called the “Statistical Modal Energy Distribution Analysis”. Here, the so called “modal interaction work” is calculated by coupling each mode of the source plate to each mode of the receiving plate [3].

The distinction of local and global modes was investigated by Hopkins [4]. He observed that considering only local modes of the uncoupled system to approximate global modes leads to unsatisfying results, although suitable boundary conditions of the junction are assumed. This aspect has been taken into account during the investigations described in this proceeding by calculating the full structure. Amongst others, Gibbs and Craven [5] investigated the influence of a variation of stiffness or plate thickness on coupled panels of concrete at frequencies higher than 100 Hz. They have shown that differences in stiffness or plate thickness can have strong influence on flanking sound transmission. In building practice, materials like concrete allow only small variations in bending stiffness, because the possible range for changing the panel thickness or Young’s Modulus is strongly limited.

Cross-laminated timber shows a high range of variations of the bending stiffness, caused by the high number of possible compositions of the panel. Here, we discuss the effect of modal (de-)coupling by numerical studies based on the finite-element-method (FEM).

## 2. Fundamental assumptions

### 2.1. Numerical calculations

The resonant structure borne sound transmission can be described by the transfer mobility between oscillating subsystems. To show the principle of this approach for coupled plates, numerical studies have been performed based on the finite element method, with a focus on flanking sound transmission. Figure 2 shows the calculation model and the chosen boundary conditions. The model contains two coupled panels, a floor and a wall forming a L-shape junction, and an air-borne sound field. The size of the room is 3 m x 3 m and the thicknesses of the panels are 0,1 m. The wall has been coupled to the air-borne sound field. The floor panel has been excited using a rain-on-the-roof excitation of the surface (unique force and arbitrary phase over the surface).

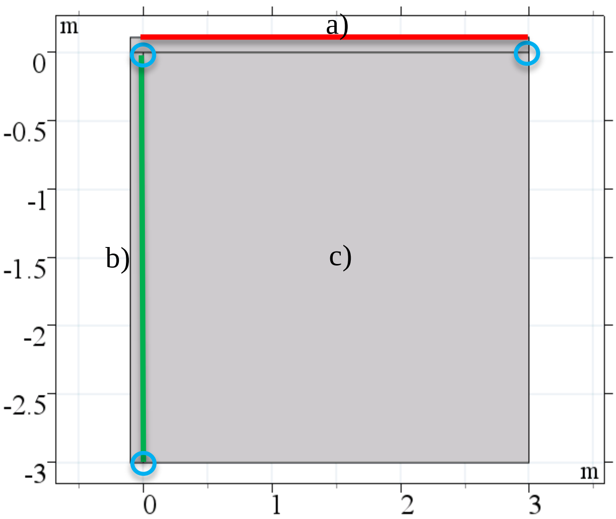


Figure 2. Geometry and boundary conditions of the calculation model for studies in the fundamental approach: a) panel 1; b) panel 2; c) air-borne sound field; fixed constraint at single points (blue); coupling of structure and air-borne sound field (green); rain-on-the-roof excitation (red)

A linear elastic, isotropic material model has been chosen to model the structure. The corresponding parameters and values are shown in Table I. A hysteretic damping with a value of 0,1 (-) has been chosen to avoid strong resonant peaks in this basic model. Quadratic shape functions have been used for the structure and the air-borne sound fields. Figure 3 shows the resulting mesh based on tetrahedron elements. A ver

Table I. Material data of the structure and of the air

| | ***Material data*** | | | |
|---|---|---|---|---|
| Parameter | ρ (kg/m³) | E (GPa) | ν (-) | c (m/s) |
| structure | 470 | 10,7 | 0,2 | - |
| air | 1,2 | - | - | 343 |

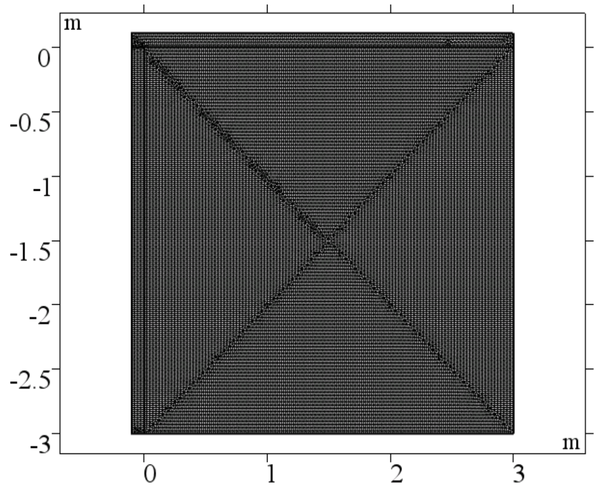


Figure 3. Resulting mesh of the calculation model for studies in the fundamental approach

The model has been studied in the frequency domain based on modal superposition of the eigenfrequencies within a frequency range of 20 Hz to 100 Hz. 5000 frequencies have been calculated using a linear distribution within the frequency range.

## 2.2. Results and discussion

Each of the subsystems in Figure 4 shows local modes. If the eigenfrequencies of two systems coincide, a global mode occurs which results in a high flanking sound transmission.

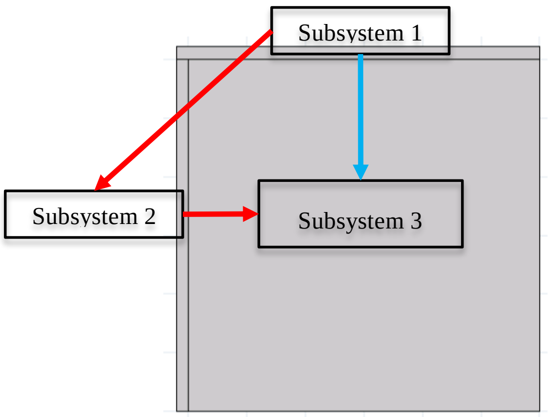


Figure 4. Resulting subsystem structure of the model for flanking sound transmission (red) and direkt sound transmission (blue)

In principle, global modes arise if the panels show the same size, boundary conditions and material data. A decoupling of the global to local modes occurs, if the properties are changed in a suitable way. We construct two extreme cases. First, the model has been solved to obtain the expected global modes using identical material parameters for the two panels. Second, the Young's modulus of panel 2 has been changed to 60 % of the one of panel 1 to reduce the influence of these global modes. For both situations, the resulting sound pressure level is evaluated. Figure 5 shows the results of the spatial averaged sound pressure level within the room, normalized to the maximum of the two situations. As discussed above, the identic sizes, boundary conditions and elastic parameters of the two panels (green graph) leads to a global mode at 57,175 Hz and results in a strong resonant peak (see also Figure 6). A reduction of the Young's modulus of panel 2 leads to a reduction of the coupling of the local modes of panel 1 and panel 2 (see also Figure 7). As a consequence, the peak of the sound pressure level in the room is decreased (blue graph).

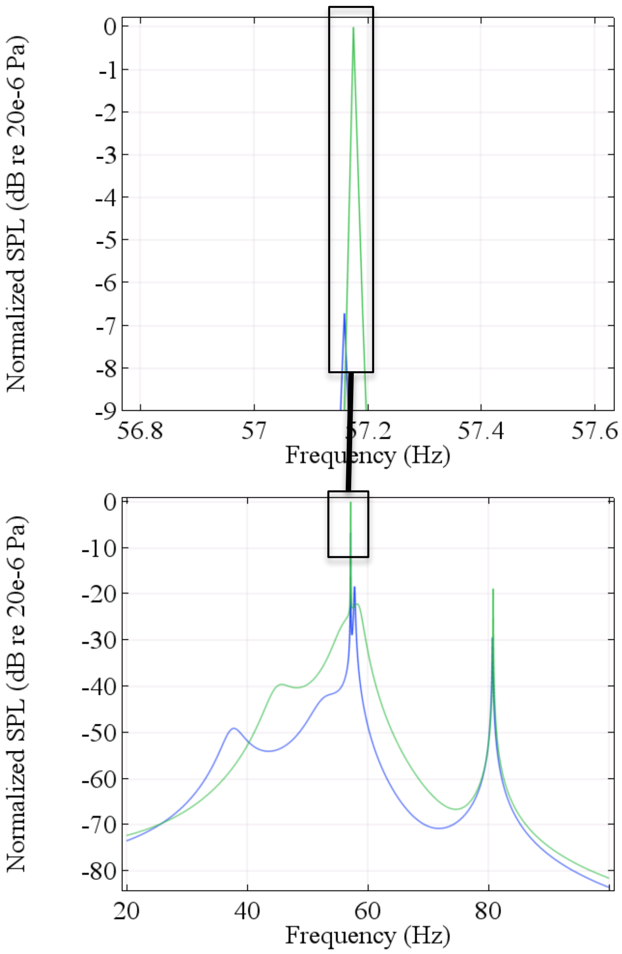


Figure 5. Normalized sound pressure level in the receiving room – results for calculations using identic Young's moduli of the two panels (green graph); results for calculations using a reduced Young's modulus for panel 2 (blue graph)

Figure 5 also shows that at low and very low frequencies, low modal density and modal overlap arise. Single resonances at defined frequencies dominate the structural and air-borne sound fields (resonant peaks in Figure 5). As mentioned before, these eigenfrequencies can have a very annoying effect on the neighbours caused by the high levels and tonal (sinusoidal) character of the noise.

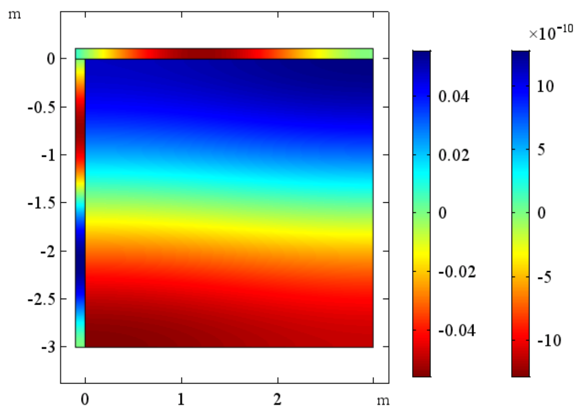

Figure 6. Global mode caused by identical panels (Frequency = 57,18 (Hz) –– left legend: total acoustic pressure field (Pa); right legend: out-of-plane displacement of the structure (m);

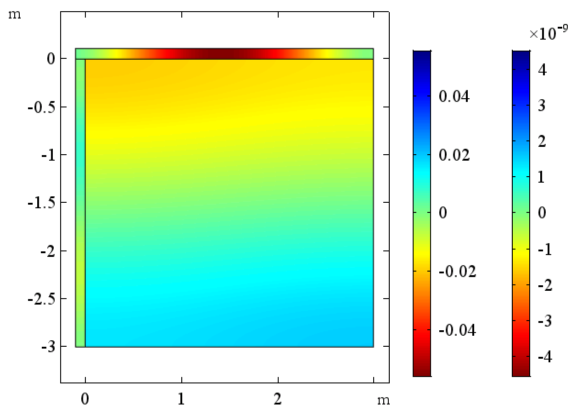

Figure 7. Decoupling of the local modes to reduce the energy transmission (Frequency = 57,16 (Hz) – left legend: total acoustic pressure field (Pa); right legend: out-of-plane displacement of the structure (m)

## 3. Application to cross-laminated timber

### 3.1. Numerical calculations

Based on the assumptions stated in the former chapter, a 3D-calculation model of two adjacent rooms has been investigated. The walls are made of panels of cross-laminated timber. The aim is to

investigate the influence of modal coupling especially to impact sound insulation.
A room with a base area of 15 m² (5 m x 3 m) and a height of 2,7 m has been implemented (base area of a typical sleeping room). Figure 8 shows the model. To allow a practical boundary condition for the junctions, the upper walls are additionally implemented to form junctions in a T-shape.

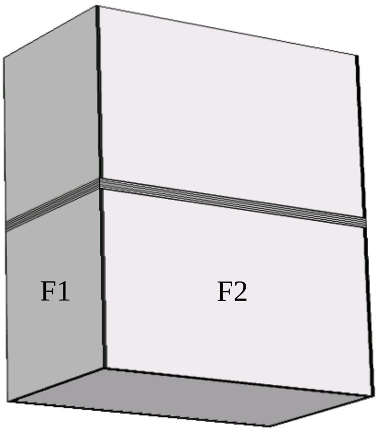


Figure 8. Calculation model of two vertical rooms based on the finite element method; F1: flanking wall 1; F2: flanking wall 2

The cross-laminated timber panels have been modelled using several continuous layers of wooden boards. The parameters of the used linear elastic, orthotropic material model are depending on the fiber orientation. Table II shows the chosen material properties, an index of 0° represent the parameters in-fiber-direction and an index of 90° represent the parameters perpendicular-to-fiber direction, as described by Kohrmann [6]. To allow a comprehensive investigation that is comparable with common used values, hysteretic damping has been implemented using a constant value of 0,01 for spruce [7].

Table II. Material data of the structure and of the air

| | *Material data* | | | |
|---|---|---|---|---|
| Parameter | $\rho$ (kg/m$^3$) | $E_{0°}/E_{90°}$ (GPa) | $\nu_{0°/90°}$ - $\nu_{90°/90°}$ (-) | c (m/s) |
| CLT [6] | 470 kg/m³ | 10,98/ 0,137 | 0,052/ 0,3 | - |
| Air | 1,2 | - | - | 343 |

To approximate several floors, the displacements on the side faces have been set equal to zero, marked in Figure 9 in red. The floor was excited using a rain-on-the-roof excitation with a unique force and an arbitrary phase. The geometry has been meshed using tetrahedron elements with a maximum element size of 0,15 m.

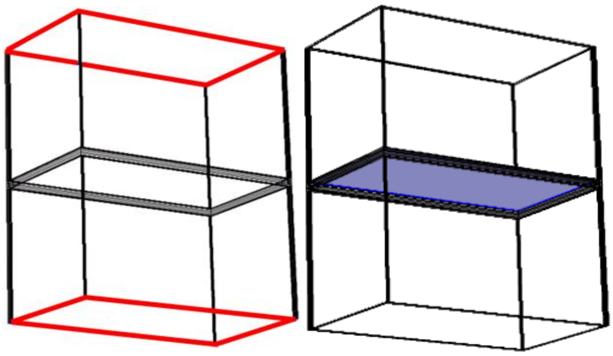

Figure 9. Fixed constraints (displacement equal to zero) to approximate rigid ceilings and floors (left); rain-on-the-roof excitation of the floor (right)

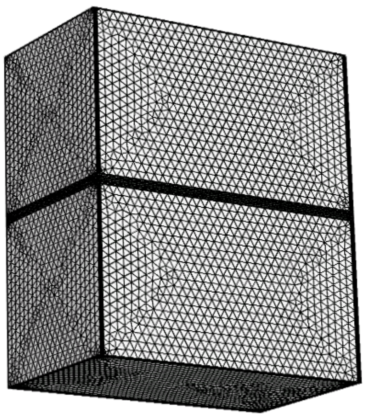

Figure 10. Resulting mesh of the geometry using thetrahedron elements

Table III. Compositions of the wall designs for parametric study

| | *Thickness (mm)* | | | | | |
|---|---|---|---|---|---|---|
| | Floor | Wall – Composition | | | | |
| Layer 1 | 34 | 19 | 27 | 30 | 40 | 19 |
| Layer 2 | 30 | 19 | 34 | 34 | 40 | 19 |
| Layer 3 | 34 | 19 | 27 | 30 | 40 | 19 |
| Layer 4 | 30 | | | | | 19 |
| Layer 5 | 34 | | | | | 19 |

The thicknesses of the layers of the flanking panels have been varied using compositions as shown in table III. The layers of the floor were constant. Every possible combination of the resulting flanking walls has been calculated in the frequency domain, based on modal superposition. The investigated frequency range was defined from 17 Hz to 113 Hz. These values are the approx. lower and upper cutoff frequencies of the one-third-octave bands at center frequencies of 20 Hz and 100 Hz. 695 Frequencies were solved using a logarithmic distribution within the frequency range.

### 3.2. Results and Discussion

The results of the calculation for the above described models show the influence of the panel composition on the formation of global modes (variable layer thicknesses in table III). Caused by the low mass and high bending stiffness of the panels of cross-laminated timber, they often show a low modal density and -overlap especially in the frequency range of 20 Hz to 100 Hz. Variations in bending stiffness lead to a shift of the eigenfrequencies of the single panel. These variations can be caused by a variation of the compositions of the single panels. Using an adjusted combination of the panels, the eigenfrequencies can be separated from each other to reduce the reaction of adjacent panels respectively the air-borne sound field, as shown in chapter 2. Table IV contains the results of a selected low-level solution (case 1) and a selected high-level solution (case 2) derived from all solutions of this parameters study.

Table IV. Comparison of a low-level (case 1) and a high-level (case 2) solution

| | *Thickness (mm)* | | | | |
|---|---|---|---|---|---|
| | Floor | Case 1 | | Case 2 | |
| | | F1 | F2 | F1 | F2 |
| Layer 1 | 34 | 19 | 27 | 30 | 40 |
| Layer 2 | 30 | 19 | 34 | 34 | 40 |
| Layer 3 | 34 | 19 | 27 | 30 | 40 |
| Layer 4 | 30 | | | | |
| Layer 5 | 34 | | | | |
| Panel | 162 | 57 | 88 | 94 | 88 |
| F1+F2 | | **145** | | **214** | |

Especially the high-level solution includes strong coupled global modes that lead to a high sound pressure level caused by resonances of the air-borne sound field.

Figure 11 shows the resulting sound pressure level in the receiving room, normalized to the maximum of the two situations within the investigated frequency range. As expected, some combinations of the parametric study result in high and some in low impact sound level. In several and especially in the two chosen cases, the aspect of modal decoupling was evident. A typical rule of thumb in building acoustics states that increasing mass leads to an increasing sound insulation. Here, additionally a different observation was made. In case 1, panels of smaller thicknesses are calculated that result in lower mass than case 2, but case 1 result in an evidently higher sound insulation than case 2. In figure 11, the mean value of the sound pressure level over the investigated frequency range is shown to allow an objective comparison. A comparison of the mean values within the investigated frequency range shows an improvement of 10,1 (dB) SPL, by using less material for the flanking walls.

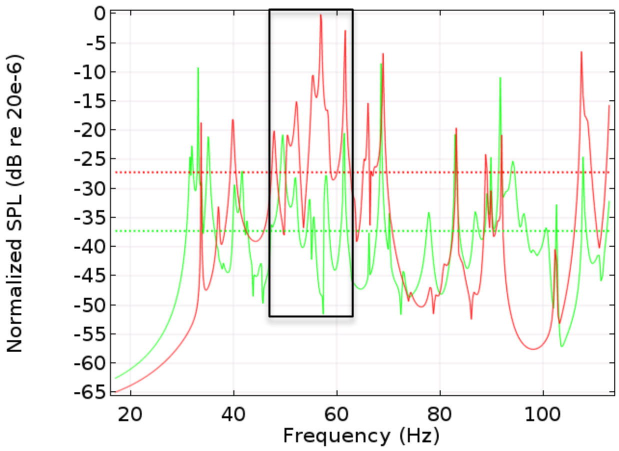


Figure 11. low-level (case 1) and high-level (case 2) solution of the parametric study – spatial averaged sound pressure level in the receiving room (–): case 1: green; case 2: red; mean values (---): case 1, green, -37.3 (dB); case 2, red, -27.2 (dB)

Within the frequency range from approx. 50 Hz to 65 Hz, case 2 shows strong resonances. Figure 12 shows the results of a detailed analysis of the two cases. A different kind of coupling of the subsystems is observed that lead to the high sound pressure in the receiving room. Caused by the same sizes of the rooms for both cases, the mode shapes and the eigenfrequencies of the room are assumed to stay constant ($a_1 – a_4$).

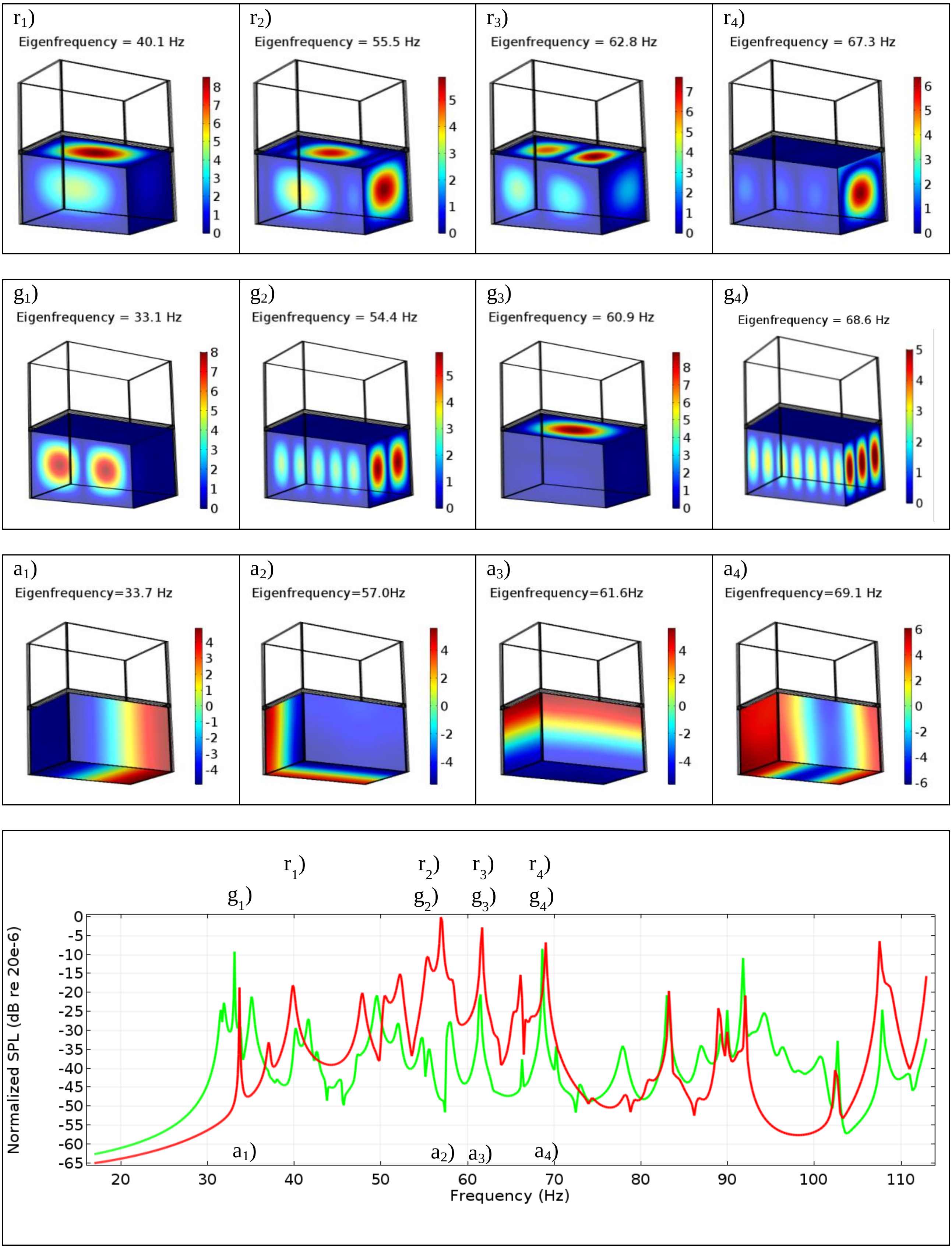


Figure 12: Detailed analysis of the different cases – Normalized sound pressure level of the case 1 (green) and the case 2 (red); Mode shapes of case 1 ($g_i$), case 2 ($r_i$), and the air-borne sound field ($a_i$)

Modes of case 1 are defined by $g_1$-$g_4$ and modes of case 2 are defined by $r_1$-$r_4$. For case 2 (red), a high level occurs in the receiving room, because on the one hand, the frequencies of structural modes are similar to one of the modes of the room. Additionally, anti-nodes of mode shapes of the structure show a high spatial correlation with anti-nodes of mode shapes of the air-borne sound field near the boundary.

This can be observed by a comparison of $r_3$ / $a_3$ for the floor (direct transmission) and by $r_4$ – $a_4$ for the flanking wall (flanking sound transmission). The structural mode $r_1$ with the frequency of 40,1 Hz differs by several Hz from resonances of the airborne sound field, $a_1$ (33,7 Hz) and $a_3$ (57,0 Hz). Compared to other resonances, this structural mode leads to a reduced sound pressure level. The highest sound pressure level is evident at nearly 57 Hz, where a strong resonance of the air-borne sound field occurs ($a_2$). This high sound pressure level is caused by the structural, global resonance at 55,5 Hz ($r_2$) that is additionally strongly coupled to the airborne sound field because of the similar eigenfrequencies. The excitation of the floor leads to a high vibration response. On the one hand, the vibration of the floor excites the airborne sound field at its resonance (direct sound transmission). On the second hand, the floor excites the flanking wall at its resonance frequency (global mode) and subsequently the flanking wall excites the airborne sound field at its resonance (flanking sound transmission).

Case 1 also shows that a high coupling of a local mode of the flanking wall ($g_1$) with the resonance of the airborne sound field ($a_1$) leads to a higher sound pressure level in the receiving room. But in contrast to case 2, the structural mode of case 1 ($g_2$) is local on both flanking walls and its eigenfrequency differs from the eigenfrequencies of the airborne sound field ($a_2$). This difference of the eigenfrequencies leads to a significant lower sound pressure level than in case 2 in the corresponding frequency range. The structural mode of $g_3$ can be assumed as local and therefore the response of the airborne sound field is reduced compared to case 2. The eigenfrequencies of modes $r_4$ and $g_4$ nearly coincide with the resonance $a_4$. Although the mode $g_4$ seems to be a global mode, this mode is not strong coupled to the (excited) floor, therefore the effect on the resulting sound pressure in the airborne-sound field is nearly comparable for both cases.

## Conclusions

Here, the impact sound insulation of constructions based on panels of cross-laminated timber at low and very low frequencies is investigated. Local modes of single components of the structure lead to global modes. An additional coupling of these global modes to the airborne sound field leads to a high sound pressure level in the room. This high level can be avoided by a suitable design of the single panels. For this purpose, the stiffness and the eigenfrequencies of panels of cross-laminated timber is modified by varying the composition of the single layers. A separation of the eigenfrequencies leads to a modal decoupling which shows a high potential for increasing the impact sound insulation especially at low and very low frequencies. Improvements of the sound insulation can be achieved by using less construction material. Further investigations will show, how the approach works using different room sizes and variations of the junctions of the CLT panels.

### Acknowledgement

The first author gratefully acknowledges funding by the Austrian Federal Ministry of Science, Research and Economy, as well as the Austrian trade association for timber within the framework of the PhD initiative “DokIn’Holz”.

### References

[1] ISO 10140-3:2015: Acoustics - Laboratory measurement of sound insulation of building elements - Part 3: Measurement of impact sound insulation. 2015.

[2] G. Müller: Beurteilung von Schallimmissionen: Gesetze – Vorschriften – Normen – Richtlinien. ed. Berlin, Heidelberg: Springer, 2017.

[3] À. Aragonès, L. Maxit, and O. Guasch: A graph theory approach to identify resonant and non-resonant transmission paths in statistical modal energy distribution analysis. Journal of Sound and Vibration, vol. 350, pp. 91-110, 2015.

[4] C. Hopkins: Structure-borne sound transmission between coupled plates. PhD Thesis, Heriot-Watt University, 2000.

[5] B. Gibbs and P. Craven: Sound transmission and mode coupling at junctions of thin plates, part II: Parametric survey. Journal of Sound and Vibration, vol. 77, pp. 429-435, 1981.

[6] M. Kohrmann: Numerical Methods for the Vibro-Acoustic Assessment of Timber Floor Constructions. PhD Thesis, Technical University of Munich, 2017.

[7] M. Möser: Technische Akustik. vol. 10, Springer, 2015.